TDOA-Based Mobile Localization Using Particle Filter With Multiple Motion and Channel Models

NAN XIA [1] **AND MARY ANN WEITNAUER**[2]**, (Senior Member, IEEE)**

[1]Dalian Polytechnic University, Dalian 116034, China
[2]College of Engineering, Georgia Institute of Technology, Atlanta, GA 30332-0250, USA

Corresponding author: Nan Xia (xianan0520@aliyun.com)

ABSTRACT Mobile terminal tracking is an important topic in wireless communications. A TDOA-based positioning method combining the interacting multiple models and the particle filter is proposed in this paper for non-cooperative target tracking in two dimensions. Three motion models, constant velocity, constant acceleration, and constant turning, and two-channel models, line of sight (LOS) and non-line of sight (NLOS), are considered to describe the trajectory of a mobile terminal in mixed LOS/NLOS environments. The particle filtering technique is employed for state estimation from a set of nonlinear TDOA measurements, and the interacting multiple models are used to mix the multiple motions and channel models to improve the accuracy of positioning. The simulation results are given to demonstrate that the proposed algorithm is close to the derived posterior Craḿer–Rao lower bound and outperforms the three-motion-model scheme with only an LOS channel model and the mixed LOS/NLOS schemes with single or two motion models. The average improvement over the whole time is larger than 40%.

INDEX TERMS Mobile terminal tracking, time difference of arrival, particle filter, interacting multiple models, posterior Craḿer-Rao lower bound (PCRLB).

I. INTRODUCTION

Mobile localization techniques have attracted much attention over the past years. Accurate positioning of an mobile terminal (MT) is very important in both commercial and military applications [1]–[4], that use various location-based services, such as emergency call service, health care monitoring, intelligent transportation, etc. In the field of radio monitoring, locating an unauthorized broadcast station in the urban environment is difficult sometimes due to severe non-line-of-sight (NLOS) observation noise. If the transmitter is mobile, the situation is even worse. In this paper, we focus on mobile tracking of a non-cooperative transmitter in urban areas.

The mobile location is determined using a set of distributed base stations (BSs). In the literature, types of BS measurements for mobile localization include time of arrival (TOA), time difference of arrival (TDOA), angle of arrival (AOA) or received signal strength (RSS). The measurements are transmitted to a data center through wireless or wired networks for information fusion. Various positioning schemes

can be found with respect to different kinds of measurements [5]–[7]. The TOA-based location scheme can measure the absolute TOA of the radio signal traveling from the MT to a certain BS. It requires exact synchronous clocks at both the transmitters and receivers, otherwise, it will lead to an imprecise location estimation [5]. The TDOA-based scheme measures the difference of TOAs of the radio signal arriving at different BSs. At least three BSs are needed to measure for a 2D location scene [6]. The AOA-based scheme uses an antenna array to measure the direction of propagation of the radio signal coming from the MT, and finds the intersection of at least two directional lines to determine the location of the MT. The receiving antenna arrays for low transmitting frequencies would be very large, which has restricted the applications of massive sensor networks [7]. The RSS-based scheme measures the power of the received radio signal to estimate the distance between the MT and BS. It has the lowest complexity and cost compared to other schemes, and can be utilized in both outdoor and indoor environments. However, the locating accuracy could be decreased due to shadowing and long distance between the target and BSs [7], [8]. Because each scheme has its own advantages and limitations, several hybrid methods are

proposed to improve the accuracy, such as TOA/RSS [8], AOA/RSS [9], TOA/AOA [10], or TDOA/AOA [11].

In urban environments, the propagation path between the MT and a BS is LOS or NLOS. The LOS measurement errors are assumed to be Gaussian [12], and the NLOS measurement errors caused by the obstruction of obstacles are frequently modeled by a shifted Gaussian distribution, exponential distribution or Nakagami distribution [13]–[15]. In [16], the TOA measurements are modeled as a random variable with a positive bias, and a modified Kalman filtering (MKF) algorithm is proposed to mitigate the effect of NLOS.

In this paper, considering both the performance and costs, we focus on the TDOA-based scheme for tracking a non-cooperative MT under the mixed LOS/NLOS conditions in two dimensions. There is a highly non-linear relationship between the TDOA measurements and MT location in the Cartesian coordinates. Usually, some modified Kalman filters [16], [17] are utilized to solve the nonlinear equations. The particle filter (PF) [18]–[20], which is based on a Bayesian framework, is another popular estimation method for nonlinear state models. In this paper, with the aim of tracking different types of MT behavior and LOS/NLOS measurement errors, we combine the PF with the interacting multiple model (IMM) algorithm [21], [22], which can mix dynamic filter models to get a better position estimate of the MT.

There have been several recent studies on mobile tracking algorithms. A fuzzy-based IMM algorithm is proposed in [23] to estimate the MT location for the urban area. The IMM algorithm is used to combine the LOS and NLOS states. The TOA and RSS measurements are employed to improve the accuracy. However, only one motion model for the MT, constant velocity, is considered. Similarly, the MKF algorithm proposed in [16] and the constrained square-root unscented Kalman filter (CSRUKF) proposed in [24] can mitigate NLOS measurement errors for tracking the MT with only constant velocity.

In practical situations, The MT may frequently speed up, slow down or make a turn. The 2D mobile target tracking with AOA measurements and the 3D mobile target tracking with TOA/AOA measurements are investigated in [25] and [26], respectively. In those papers, the interacting multiple model unscented Kalman filter (IMMUKF), IMMEKF, and IMMPF algorithms are proposed for tracking the MT with three dynamic motion models. However, the algorithms only work well under LOS conditions. A two-stage Kalman-based tracking algorithm is proposed in [27], where the onboard sensors measure distance, velocity and heading. These measurements are sent to the BSs and are used to mitigate the NLOS measurement errors. However, for non-cooperative tracking, this sensed information is not available at the BSs.

In this paper, three different motion models, constant velocity (CV), constant acceleration (CA), and constant turning (CT) are considered, and the LOS/NLOS measurement noise is modeled as mixed Gaussian distribution according to [13]. An improved IMMPF algorithm is proposed, which

can combine the motion and channel models to achieve accurate location estimation of the MT in urban areas.

The paper contributes more than just a straightforward combination of multiple motion and multiple channel models. The contributions are summarized as follows:

- For each motion model, we estimate distance difference offsets and the channel model probability to combine the channel state estimates. With the compensation of channel parameters, the estimation accuracy of motion states is improved. Then, we calculate the likelihood probability to update the state estimates and the corresponding covariances.
- We present the PCRLB for theoretical performance analysis. Compared with [25], we derive the lower bound with a new treatment required because of nonzero expectation of residual error and the different offsets.
- We design a new simulation scenario, where the target moves with three different motion models and in the mixed LOS/NLOS environment. The results show that the proposed algorithm outperforms other compared schemes, in which one or more of the models e.g., NLOS or CT is left out.

The remainder of this paper is organized as follows. Section II introduces the system model, motion model, measurement and channel model. Section III describes the proposed IMMPF algorithm. In Section IV, the posterior CRLB is derived. The numerical simulations of the localization performance are analyzed in Section V. Finally, Section VI gives a brief conclusion about this paper.

II. SYSTEM MODEL

Focusing on mobile localization in the mixed LOS/NLOS channel environment, the state-space model of the tracking system in this paper is represented as

$$x(k + 1) = f(x(k)) + w(k) \qquad (1)$$
$$z(k) = h(x(k)) + v(k) \qquad (2)$$

where k is the time index, $x(k)$ is the state vector, $z(k)$ is the measurement vector, and $f(\cdot)$ and $h(\cdot)$ are the state transition and measurement function, respectively. $w(k)$ denotes the process noise vector, and $v(k)$ denotes the measurement noise vector.

The state vector $x(k)$ including motion and channel states is defined as

$$x(k) = [x_t(k); x_L(k); x_N(k)], \qquad (3)$$

where

$$x_t(k) = [x(k), \dot{x}(k), \ddot{x}(k), y(k), \dot{y}(k), \ddot{y}(k)]^T$$
$$x_L(k) = \left[\Delta d_{L,1}(k), \dots, \Delta d_{L,m}(k), \dots, \Delta d_{L,M-1}(k)\right]^T$$
$$x_N(k) = \left[\Delta d_{N,1}(k), \dots, \Delta d_{N,m}(k), \dots, \Delta d_{N,M-1}(k)\right]^T.$$

$x(k)$, $\dot{x}(k)$ and $\ddot{x}(k)$ denote the target position, velocity and acceleration, respectively, in the horizontal axis. $y(k)$, $\dot{y}(k)$ and $\ddot{y}(k)$ denote the same physical elements in the vertical axis. $x_L(k)$ and $x_N(k)$ are distance difference offset vectors

at time index k under LOS and NLOS conditions, respectively. The elements $\Delta d_{L,m}(k)$ and $\Delta d_{N,m}(k)$ denote the distance difference offset of the m-th channel state under LOS and NLOS conditions, respectively. In this paper, the offsets are modeled as the mean values of the LOS and NLOS measurement noise, respectively. They are used to track channel switching. M is the number of BSs.

For the motion state $x_t(k)$, three typical motion models, CV, CT and CA, are considered, as described in [25]

$$f_j(x_t(k)) = F_{t,j} \cdot x_t(k), \quad j = 1, 2, 3 \tag{4}$$

where $j = 1, 2, 3$ denote the indexes of CV, CT and CA motion model, respectively. The state transition matrixes are expressed by

$$F_{t,1} = I_2 \otimes \begin{bmatrix} 1 & T & 0 \\ 0 & 1 & 0 \\ 0 & 0 & 0 \end{bmatrix}, \tag{5}$$

$$F_{t,2} = \begin{bmatrix} 1 & \dfrac{\sin(\omega T)}{\omega} & 0 & 0 & \dfrac{\cos(\omega T) - 1}{\omega} & 0 \\ 0 & \cos(\omega T) & 0 & 0 & -\sin(\omega T) & 0 \\ 0 & 0 & 0 & 0 & 0 & 0 \\ 0 & \dfrac{1 - \cos(\omega T)}{\omega} & 0 & 1 & \dfrac{\sin(\omega T)}{\omega} & 0 \\ 0 & \sin(\omega T) & 0 & 0 & \cos(\omega T) & 0 \\ 0 & 0 & 0 & 0 & 0 & 0 \end{bmatrix}, \tag{6}$$

$$F_{t,3} = I_2 \otimes \begin{bmatrix} 1 & T & \dfrac{T^2}{2} \\ 0 & 1 & T \\ 0 & 0 & 1 \end{bmatrix}, \tag{7}$$

where T denotes the sampling interval, ω denotes the turning rate, which is also treated as an auxiliary parameter to be estimated in this paper [25], [28]. Therefore, the motion model state of Equation (3) can be rewritten as $x_t(k) = [x(k), \dot{x}(k), \ddot{x}(k), y(k), \dot{y}(k), \ddot{y}(k), \omega]^T$. The process noise covariance matrix Q_j could be found in [25].

For the channel state, two channel models, LOS and NLOS, are considered. The states are also modeled as random processes with the state transition function

$$\begin{cases} f_L(x_L(k)) = x_L(k), \\ f_N(x_N(k)) = x_N(k). \end{cases} \tag{8}$$

The corresponding noise process covariance matrices are Q_L and Q_N, respectively. This assumption is reasonable as the channel states are relatively stable for a mobile target with moderate speed.

Combining equation (4) and (8), we can obtain the transition function of equation (1),

$$f_j(x(k)) = \begin{bmatrix} F_{t,j} & 0 \\ 0 & I_{2M-1} \end{bmatrix} \cdot x(k). \tag{9}$$

$z(k)$ is the measurement vector of distance difference. Assume that there are $M (M \geq 3)$ BSs with fixed locations to detect the signal transmitted from the target. The TDOA measurements of the transmitted signals are collected by a set
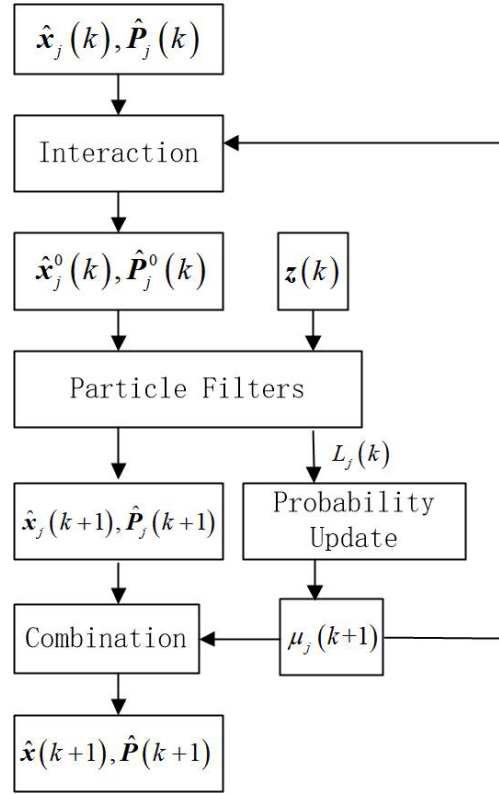

FIGURE 1. The traditional IMMPF algorithm.

of BSs with a common reference. The measurement vector is expressed by $z(k) = c \left[\tau_{2,1}(k), \ldots, \tau_{m,1}(k), \ldots, \tau_{M,1}(k) \right]^T$, where c is speed of light, $\tau_{m,1}(k)$ is the TDOA between base station BS_m and the reference BS_1 at time index k. Thus, given a set of distance values between the target and each BS $[d_1, \ldots, d_m, \ldots, d_M]^T$, the observation equation can be expressed by

$$z(k) = d + v(k), \tag{10}$$

where $d = \left[d_{2,1}, \ldots, d_{m,1}, \ldots, d_{M,1} \right]^T$ is the distance difference vector and the element is $d_{m,1} = d_m - d_1$. $v(k)$ denotes the LOS/NLOS measurement noise vector. According to [13] and [14], the element $v_m(k)$ is modeled by Gaussian mixture PDF, which can be written in a general form as follows:

$$v_m(k) \sim \begin{cases} \mathcal{N}\left(0, \sigma_{L,m}^2\right), & LOS \\ \mathcal{N}\left(\Delta d_m, 2\sigma_{L,m}^2 + \sigma_{N,m}^2\right). & NLOS \end{cases} \tag{11}$$

Under the LOS condition, the measurement noise is modeled as an independent and identically distributed (*iid*) zero-mean Gaussian variables with the distribution $\mathcal{N}\left(0, \sigma_{L,m}^2\right)$. Under the NLOS condition, the measurement noise is modeled as an *iid* positive-mean Gaussian variables with the distribution $\mathcal{N}\left(\Delta d_m, \sigma_{N,m}^2\right)$, where Δd_m represents the distance difference offset. In symbols, $\Delta d_m = E\left\{ z_m(k) - d_{m,1} \right\}$. Δd_m is a time-invariant parameter required to be estimated in this paper. $\Delta d_m \gg 0$, $\sigma_{N,m}^2 > \sigma_{L,m}^2$.
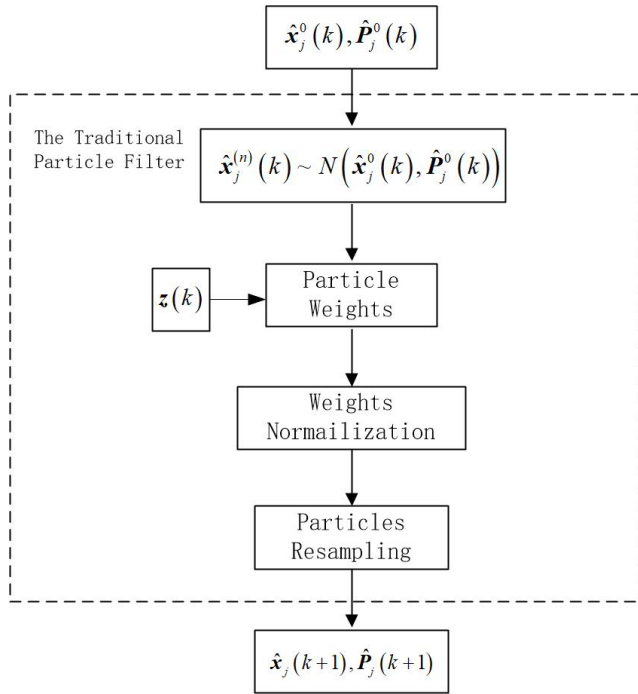
FIGURE 2. The traditional particle filtering algorithm.

III. THE IMPROVED IMMPF ALGORITHM

In this paper, the motion and channel states are described by the three-model and two-model dynamics of the state equations, respectively. The IMM algorithm can track the MT by switching models according to transition probabilities driven by Markov jump process. The PF technique is introduced to estimate nonlinear parameters.

In general, the traditional particle filtering-based IMM algorithm consists of four major stages, as shown in Fig.1. 1) Interaction. Based on the mode probability $\mu_i(k)$ at time index k, the initial state vector estimate $\hat{x}_j^0(k)$ and the corresponding covariance matrix $\hat{P}_j^0(k)$ are obtained by mixing the state estimate $\hat{x}_j(k)$ and the state error covariance $\hat{P}_j(k)$ of the previous iteration. 2) State update. With the use of the initial state estimate and the covariance, as well as the measurement data $z(k)$, the new state estimate $\hat{x}_j(k + 1)$ and covariance $\hat{P}_j(k + 1)$ are obtained from a set of parallel particle filters. 3) Mode probability update. By using the measurement residual, the likelihood function $L_j(k)$ is calculated, and the new mode probability $\mu_j(k + 1)$ can be updated. 4) Combination. All the state estimates and their corresponding covariances are mixed to obtain $\hat{x}(k+1)$ and $\hat{P}(k+1)$. The particle filtering algorithm used in the IMMPF is summarized in Fig.2.

Compared with the traditional IMMPF algorithm, the improvement of the proposed algorithm is made in the state update block as shown in Fig.3, where both LOS and NLOS channel parameters are estimated to reduce the effect of large NLOS measurement errors and the traditional particle filtering algorithm is replaced by the filtering and resampling block. First, particles $\hat{x}_j^{(n)}(k)$ are obtained from the initial

distribution at time index k for each motion model, where the index n denote the n-th particle. Then, by using the measurement residual, the likelihood coefficient $\varepsilon_{j,i,m}(k)$ and the channel probability $\eta_{j,i,m}(k)$ are computed to combine all the channel state estimates, where the index j, i and m denote the j-th motion model, the i-th channel model and the m-th path, respectively. Note that $i = 1$ and $i = 2$ denote LOS and NLOS conditions, respectively. The particles of channel states need to be reset if the channel switches from model LOS to NLOS, which is determined by comparing the channel probabilities. Otherwise, the state $\hat{x}_j(k + 1)$ is directly obtained based on particle resampling. The details of the proposed algorithm are described as follows.

Compared to the motion-model-only schemes, the proposed algorithm considers both motion and channel models. The channel model probability is calculated to mix LOS and NLOS channel measurement errors. The algorithm firstly samples particles from the initial distribution

$$\hat{x}_j^{(n)}(k) \sim \mathcal{N}\left(\hat{x}_j^0(k), \hat{P}_j^0(k)\right), \quad (12)$$

where $n = 1, 2, \ldots, N_p$ and N_p is the number of particles. The predicted state particles of the j-th motion model could be obtained by

$$\hat{x}_j^{(n)}(k + 1) = f_j\left(\hat{x}_j^{(n)}(k)\right) + w_j(k). \quad (13)$$

Using the distance difference equation of (10), the measurement errors can be expressed as

$$e_{j,i,m}^{(n)}(k + 1) = z_m(k + 1) - d_{m,1}^{(n)}(k + 1) - \Delta\hat{d}_{j,i,m}^{(n)}(k + 1), \quad (14)$$

where $e_{j,i,m}^{(n)}(k+1)$ denotes the measurement error. $\Delta\hat{d}_{j,i,m}^{(n)}(k+1)$ denotes the offset of the distance difference $d_{m,1}^{(n)}(k + 1)$; it is an element of $\hat{x}_j^{(n)}(k + 1)$ and it has the mean value of the distribution as shown in Equation (11). $z_m(k + 1)$ is the distance difference measurement. Then, the likelihood probability coefficient can be calculated as

$$\varepsilon_{j,i,m}(k + 1) = \frac{1}{\sqrt{2\pi\sigma_{j,i,m}^2(k+1)}} \exp\left(-\frac{\left|\bar{e}_{j,i,m}(k+1)\right|^2}{2\sigma_{j,i,m}^2(k+1)}\right), \quad (15)$$

where the mean and covariance are defined as

$$\bar{e}_{j,i,m}(k + 1) = \frac{1}{N_p} \sum_{n=1}^{N_p} e_{j,i,m}^{(n)}(k + 1), \quad (16)$$

$$\sigma_{j,i,m}^2(k + 1) = \frac{1}{N_p} \sum_{n=1}^{N_p} \left|e_{j,i,m}^{(n)}(k + 1)\right|^2. \quad (17)$$

The mixed measurement errors and variance can be calculated by

$$\tilde{e}_{j,m}^{(n)}(k + 1) = z_m(k + 1) - d_{m,1}^{(n)}(k + 1) - \sum_{i=1}^{2} \eta_{j,i,m}(k + 1)\Delta\hat{d}_{j,i,m}^{(n)}(k + 1) \quad (18)$$

and

$$\sigma_{j,m}^2(k+1) = \frac{1}{N_p} \sum_{n=1}^{N_p} \left| \tilde{e}_{j,m}^{(n)}(k+1) \right|^2, \qquad (19)$$

where the channel model probability coefficient $\eta_{j,i,m}(k+1)$ is calculated with the following equations,

$$\eta_{j,i,m}(k+1) = \frac{1}{c'_{j,m}(k)} \varepsilon_{j,i,m}(k+1) c'_{j,i,m}(k), \qquad (20)$$

$$c'_{j,i,m}(k) = \sum_{i'=1}^{2} \varphi_{i'i} \eta_{j,i,m}(k), \qquad (21)$$

$$c'_{j,m}(k) = \sum_{i=1}^{2} c'_{j,i,m}(k), \qquad (22)$$

where $\varphi_{i'i}$ is the element of the assumed transition probability matrix Ψ and $\eta_{j,i,m}(k)$ is the channel model probability. It is obvious that $\eta_{j,2,m}(k)$ is much larger than $\eta_{j,1,m}(k)$ if the channel switches from model LOS to NLOS. Given a threshold Pr, the channel particles should be reset for the new estimates of channel parameters according to Fig.3. With the combination of two channel models, the mixed measurement errors are computed. Therefore, the particle sampling weights are obtained by

$$w_j^{(n)}(k+1) = w_j^{(n)}(k) \prod_{m=1}^{M-1} w_{j,m}^{(n)}(k+1), \qquad (23)$$

where

$$w_{j,m}^{(n)}(k+1) = \frac{1}{\sqrt{2\pi\sigma_{j,m}^2(k+1)}} \exp\left(-\frac{\left| \tilde{e}_{j,m}^{(n)}(k+1) \right|^2}{2\sigma_{j,m}^2(k+1)} \right). \qquad (24)$$

The initial weights are set to $w_j^{(n)}(0) = 1/N_p$. The weights should be normalized as

$$\bar{w}_j^{(n)}(k+1) = \frac{w_j^{(n)}(k+1)}{\sum_{n=1}^{N_p} w_j^{(n)}(k+1)}. \qquad (25)$$

Based on the existing resampling scheme [17], the particles are updated, the new state estimates and the corresponding covariance matrix can be computed as

$$\hat{x}_j(k+1) = \sum_{n=1}^{N_p} \bar{w}_j^{(n)}(k+1) \hat{x}_j^{(n)}(k+1), \qquad (26)$$

$$\hat{P}_j(k+1) = Q_j + \sum_{n=1}^{N_p} \bar{w}_j^{(n)}(k+1) \hat{X}_j^{(n)}(k+1) \left(\hat{X}_j^{(n)}(k+1) \right)^T, \qquad (27)$$

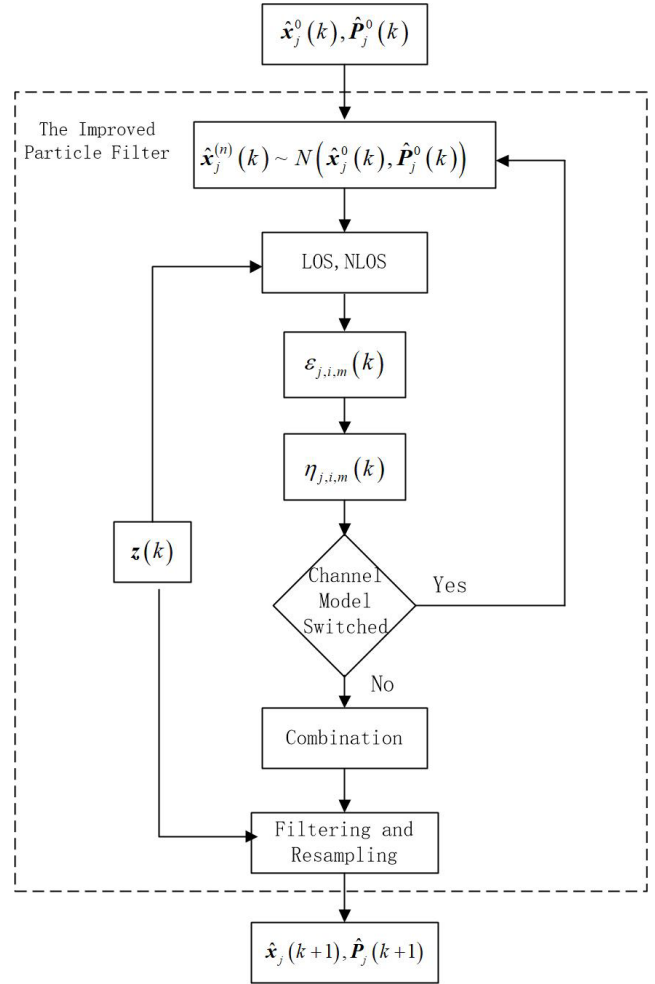where $\hat{X}_j^{(n)}(k+1) = \hat{x}_j^{(n)}(k+1) - \hat{x}_j(k+1)$.

FIGURE 3. The improved particle filtering algorithm.

IV. POSTERIOR CRLB

In the mobile target tracking system, the parameter vector is modeled as a random vector. Therefore, we consider the posterior CRLB, which is defined as the inverse of the Fisher information matrix (FIM) for a random vector and is a very important tool for nonlinear filtering problems [29], [30]. The posterior CRLB of the estimation error covariance for motion model j is

$$E\left[\left(\hat{x}_j(k) - x(k) \right) \left(\hat{x}_j(k) - x(k) \right)^T \right] \geq J_j^{-1}(k). \qquad (28)$$

The FIM $J_j^{-1}(k)$ can be recursively calculated by

$$J_j(k+1) = D_j^{22}(k) - D_j^{21}(k) \left(J_j(k) + D_j^{11}(k) \right)^{-1} D_j^{12}(k), \qquad (29)$$

The difference between the proposed posterior CRLB and the derivations in the literature [25] is the calculation of $D_j^{22}(k)$. The literature assumes that the expectation of the residual measurement errors is zero, while the expectation in this paper is nonzero due to the influence of the distance

difference offsets. Therefore, $D_j^{22}(k)$ can be written as

$$
\begin{aligned}
D_j^{22}(k) &= E\left\{-\Delta_{x_j(k+1)}^{x_j(k+1)} \log p\left(x_j(k+1)|x_j(k)\right)\right\} \\
&\quad + E\left\{-\Delta_{x_j(k+1)}^{x_j(k+1)} \log p\left(z_j(k+1)|x_j(k+1)\right)\right\} \\
&= Q_j^{-1} + H_j^T(k+1)R_j^{-1}(k+1)H_j(k+1) \\
&\quad - \tilde{H}_j^T(k+1)\tilde{R}_j^{-1}(k+1)B_j(k+1), \quad (30)
\end{aligned}
$$

where symbol $\triangle$ denotes the second-order derivative operator. Using the measurement model shown in Equation (18), the matrix $H_j(k+1)$ can be expressed by Equation (31), as shown at the bottom of this page, where

$$
\begin{aligned}
&x_j^{m+1,1}(k+1) \\
&= \frac{\left(x_j(k+1)-\alpha_m\right)}{\sqrt{\left(x_j(k+1)-\alpha_m\right)^2 + \left(y_j(k+1)-\beta_m\right)^2}} \\
&\quad - \frac{\left(x_j(k+1)-\alpha_1\right)}{\sqrt{\left(x_j(k+1)-\alpha_1\right)^2 + \left(y_j(k+1)-\beta_1\right)^2}} \quad (32)
\end{aligned}
$$

$$
\begin{aligned}
&y_j^{m,1}(k+1) \\
&= \frac{\left(y_j(k+1)-\beta_m\right)}{\sqrt{\left(x_j(k+1)-\alpha_m\right)^2 + \left(y_j(k+1)-\beta_m\right)^2}} \\
&\quad - \frac{\left(y_j(k+1)-\beta_1\right)}{\sqrt{\left(x_j(k+1)-\alpha_1\right)^2 + \left(y_j(k+1)-\beta_1\right)^2}}, \quad (33)
\end{aligned}
$$

and (α_m, β_m) denotes the position coordinate of the m-th BS. The measurement covariance matrix $R_j(k+1)$ can be expressed by

$$
R_j(k+1) = diag\left[\sigma_{j,2}^2(k+1), \ldots, \sigma_{j,M}^2(k+1)\right] \quad (34)
$$

where $\sigma_{j,m}^2(k+1)$ is calculated by Equation (19). $\tilde{H}_j(k+1)$ is a $((M-1)(2M+5)) \times (2M+5)$ matrix, has

$$
\tilde{H}_j(k+1) = \nabla_{x_j(k+1)} H_j(k+1) \quad (35)
$$

where ∇ denotes the gradient operator. $\tilde{R}_j(k+1)$ is a $((M-1)(2M+5)) \times ((M-1)(2M+5))$ matrix, defined as

$$
\tilde{R}_j(k+1) = R(k+1) \otimes I_{(2M+5)\times(2M+5)} \quad (36)
$$

where $\otimes$ denotes the Kronecker product. $B_j(k+1)$ is a $((M-1)(2M+5)) \times (2M+5)$ matrix, defined as

$$
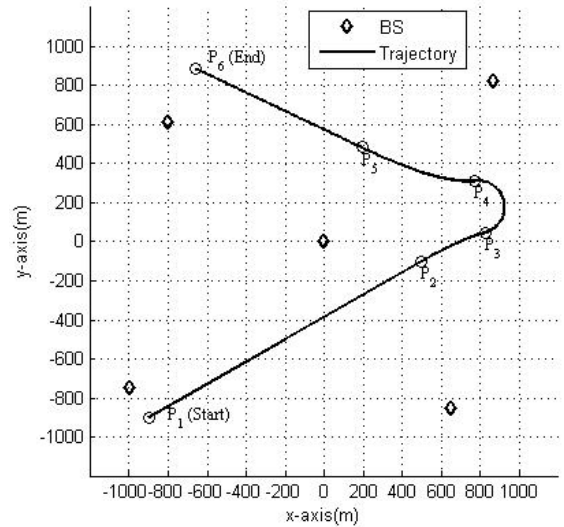B_j(k+1) = \tilde{E}_j(k+1) \otimes I_{(2M+5)\times(2M+5)} \quad (37)
$$

FIGURE 4. The mobile target trajectory in a BS wireless sensor network, special case for $M = 5$.

where $\tilde{E}_j(k+1)$ is calculated according to Equation (18),

$$
\tilde{E}_j(k+1) = \frac{1}{N_p}\left[\sum_{n=1}^{N_p} \tilde{e}_{j,2}^{(n)}(k+1), \ldots, \sum_{n=1}^{N_p} \tilde{e}_{j,M}^{(n)}(k+1)\right]^T \quad (38)
$$

V. SIMULATION RESULTS

In our simulations, the proposed algorithm is assessed according to the scenario shown in Fig. 4. We assume that both the BS locations and the mobile target trajectory are in a region of size 2×2 km^2. The reference BS is placed at the center of the region $(0, 0)$, and the other $M-1$ BSs are randomly deployed. The time series data collected simultaneously from different sensors are uploaded to a fusion center for distance difference values calculation. The sampling interval is $T = 1s$, and the total sampling duration is equal to 550s. We assume that all the BSs are active and able to sense the information from the mobile transmitter during the whole sampling period. Three different motion models [25] are used to describe the trajectory of a mobile target. The trajectory starts at point P_1 with an initial velocity $(7m/s, 4m/s)$ and an initial acceleration $(0, 0)$. During the first 200 samples, the mobile target travels at the initial constant speed, and

$$
\begin{aligned}
&H_j(k+1) \\
&= \frac{\partial \log\left(p\left(z(k+1)|x_j(k+1)\right)\right)}{\partial x_j(k+1)} \\
&= \begin{bmatrix}
x_j^{2,1}(k+1) & 0 & 0 & y_j^{2,1}(k+1) & 0 & 0 & 0 & \eta_{j,1,1}(k+1) & \cdots & 0 & \eta_{j,2,1}(k+1) & \cdots & 0 \\
\vdots & \vdots & \vdots & \vdots & \vdots & \vdots & \vdots & \vdots & \ddots & \vdots & \vdots & \ddots & \vdots \\
x_j^{M,1}(k+1) & 0 & 0 & y_j^{M,1}(k+1) & 0 & 0 & 0 & 0 & \cdots & \eta_{j,1,M-1}(k+1) & 0 & \cdots & \eta_{j,2,M-1}(k+1)
\end{bmatrix} \quad (31)
\end{aligned}
$$

arrives at the point P_2. From the 201th sample to the 260th sample, the mobile target slows down with a constant acceleration, $(-0.05m/s^2, -0.05m/s^2)$, and reaches the point P_3. From the 261th sample to the 360th sample, the target makes a turn with a constant rate of $0.03rad/s$ until it arrives at the point P_4. Then, from the 361th sample to the 450th sample, the target speeds up with a constant acceleration of $(0.05m/s^2, 0.05m/s^2)$. After passing through the point P_5, from the 451th sample to the 550th sample, the target keeps the constant speed and finally arrives at the point P_6. With regard to channel models, Reference [24] change the sight condition every 250 samples. This paper made an improvement of the channel model. The LOS or NLOS channel model of each BS is changed independently with the switching rate λ. The switching time vector of the total sampling duration is generated by *iid* uniform random variables, as

$$\tau \sim 550 \cdot \mathcal{U}(1, \lambda), \qquad (39)$$

The parameters used in this paper are given as follows. The standard deviation of LOS and NLOS measurement noise in Equation (11) are $\sigma_{L,m+1} = 10m$ and $\sigma_{N,m+1} = 100m$, respectively, and the positive mean is assumed to be in the range of $[300m, 800m]$. The initial state vector is $\hat{x}(0) = 0_{(2M+4)\times1}$. The number of particles is $N_p = 500$. The initial motion model probability described in Fig.1 is $\mu_j(0) = 1/3$ and the transition matrix, used to update the probability, is

$$\Pi = \begin{bmatrix} 0.70 & 0.15 & 0.15 \\ 0.15 & 0.70 & 0.15 \\ 0.15 & 0.15 & 0.70 \end{bmatrix}.$$

The initial channel model probability is $\eta_{j,i,m}(0) = 1/2$ and the transition matrix used in equation (17) is

$$\Psi = \begin{bmatrix} 0.99 & 0.01 \\ 0.01 & 0.99 \end{bmatrix}.$$

Since the transition probability of model NLOS is 0.99, we are able to set the threshold $Pr = 0.9$ for NLOS condition identification in Fig.2. The initial particles are drawn from the following distribution

$$x_j^{(n)}(1, 0), \ x_j^{(n)}(4, 0) \sim \mathcal{U}(-1000m, 1000m),$$
$$x_j^{(n)}(2, 0), \ x_j^{(n)}(5, 0) \sim \mathcal{U}(-10m/s, 10m/s),$$
$$x_j^{(n)}(3, 0), \ x_j^{(n)}(6, 0) \sim \mathcal{U}(-1m^2/s, 1m^2/s),$$
$$x_j^{(n)}(7, 0) \sim \mathcal{U}(0, 1rad/s),$$
$$x_j^{(n)}(8 : 6+M, 0) \sim \mathcal{U}(100m, 1000m),$$
$$x_j^{(n)}(7+M : 2M+5, 0) \sim \mathcal{U}(100, 1000m).$$

Fig.5 and Fig.6 show the target positions and distance difference offsets estimation with the proposed algorithm, respectively. In this simulation trial, the number of BSs is 5 and the switching rate is 4. The dashed lines represent the estimation results. It can be seen that the channel states are totally different from each other but they are accurately
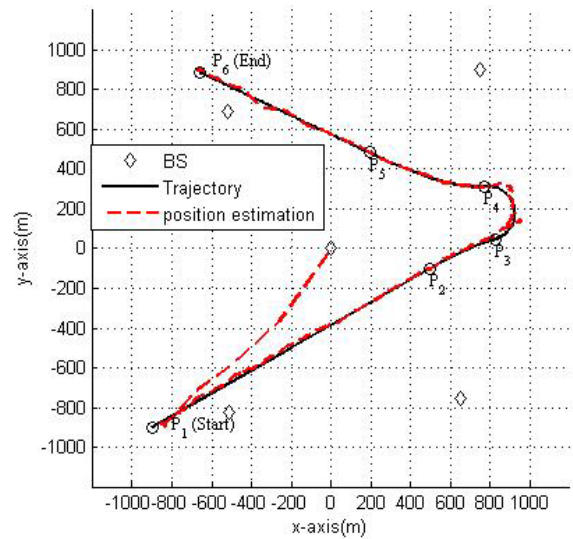

FIGURE 5. The position estimation of a mobile target in a single simulation trial, special case for $M = 5$, $\lambda = 4$.
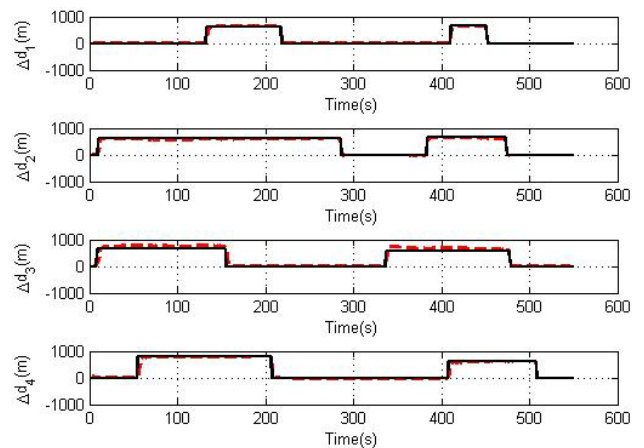

FIGURE 6. The estimation of distance difference offsets in a single simulation trial, special case for $M = 5$, $\lambda = 4$.

recovered. Therefore, with the compensation of distance difference offsets, the proposed algorithm could provide robust performance for complicated conditions.

To assess the performance of position estimation and distance difference offset tracking, the root mean square error (RMSE) with 50 Monte Carlo simulations is calculated. The RMSE of position estimation is defined as

$$E_p(k) = \sqrt{\frac{1}{50} \sum_{l=1}^{50} \left[\left(\hat{x}_l(k) - x(k)\right)^2 + \left(\hat{y}_l(k) - y(k)\right)^2 \right]}, \qquad (40)$$

where $\hat{x}_l(k)$ and $\hat{y}_l(k)$ are the position estimate in the l-th trial at the k-th time sample for the x and y axes, respectively, and $x(k)$ and $y(k)$ are the actual position of the target. The RMSE
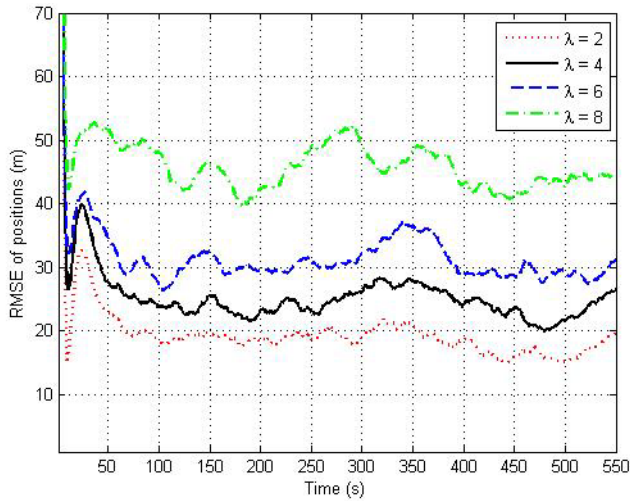
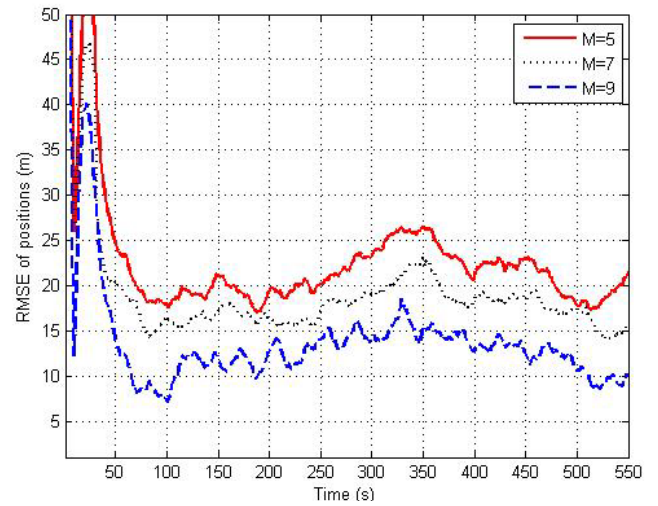**FIGURE 7.** Comparison of position estimation versus different channel switching rate λ, the number of BSs *M* = 5.
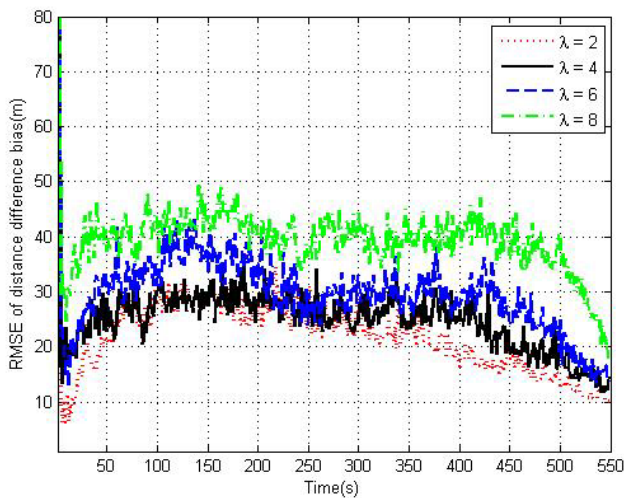

FIGURE 8. Comparison of distance difference offset estimation versus different channel switching rate λ, the number of BSs *M* = 5.

FIGURE 9. Comparison of position estimation versus different number of BSs *M*, the channel switching rate λ = 4.

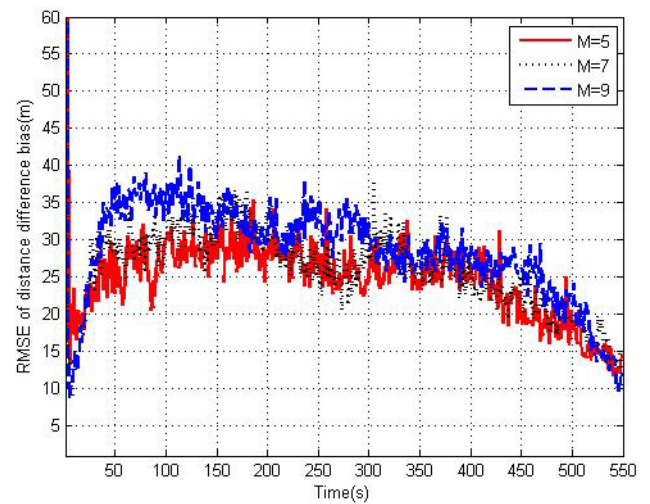**FIGURE 10.** Comparison of distance difference offset estimation versus different number of BSs *M*, the channel switching rate λ = 4.

of distance difference offset tracking is defined as

$$E_d(k) = \sqrt{\frac{1}{50}\frac{1}{M-1}\sum_{l=1}^{50}\sum_{m=1}^{M-1}\left(\Delta\hat{D}_{m,l}(k) - \Delta D_m(k)\right)^2},$$

(41)

where $\Delta\hat{D}_{m,l}(k)$ denotes the estimation of distance difference offset of the m-th path in the l-th trial at the k-th time sample, and $\Delta D_m(k)$ denotes the actual LOS/NLOS mixed distance difference offset.

In the first simulation test, 5 BSs are employed to track the target. The position and distance difference offset RMSEs of the proposed algorithm are shown in Fig.7 and Fig.8, respectively. The errors are compared with different channel model switching rate. Obviously, with the increase of the rate, the estimation performance of the proposed algorithm is degraded. For the condition of λ = 4, the LOS/NLOS model switching and the CT/CA motion model switching

occur simultaneously during the sampling time from 300*s* to 450*s*, which makes the estimation errors of both position and distance difference offset larger than that of the condition of λ = 2. For the conditions of λ = 6 and λ = 8, the estimation accuracy is reduced significantly because the frequently switched channel model introduces more measurement noise.

Next, the position and distance difference offset estimation with different numbers of BSs are shown in Fig.9 and Fig.10, respectively. It is known that the TDOA-based localization algorithms require at least 3 BSs to find the position of the target. However, in the mixed LOS/NLOS environment, more BSs are required to improve the locating performance. In this simulation test, we compare the RMSEs with $M = 5, 7, 9$. In Fig.9, the algorithm with 9 BSs outperforms the other algorithms, especially for the time duration from 300*s* to 450*s*, because more distance measurements can reduce the
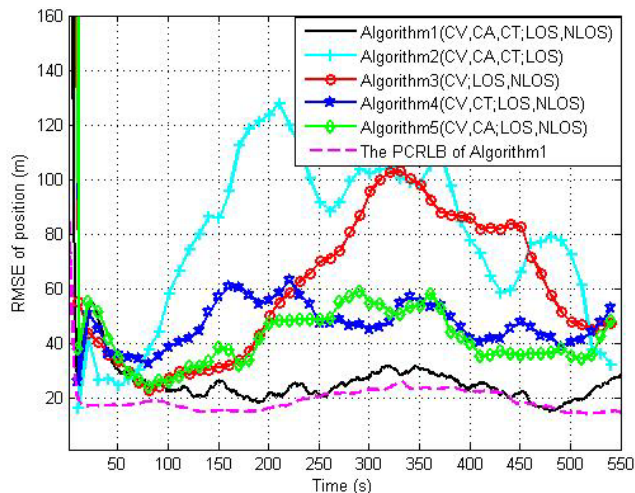
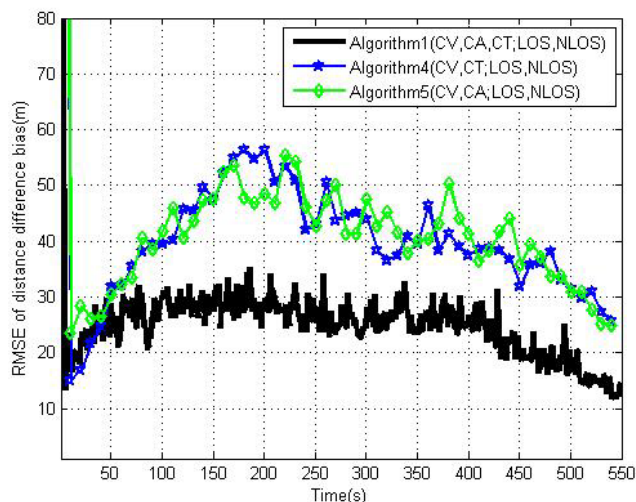**FIGURE 11.** Comparison of position estimation, the channel switching rate λ = 4, the number of BSs *M* = 5.

FIGURE 12. Comparison of distance difference offset estimation, the channel switching rate λ = 4, the number of BSs *M* = 5.

tracking errors of the target whose motion model is switched from one to another. However, in Fig.10, the RMSEs of the distance difference offset are close. Equation (41) demonstrates that the RMSE is not sensitive to the number of BSs. Considering both system complexity and locating accuracy, it is reasonable to use 5 BSs for mobile target tracking. In the real-world case, the data utilization depends on the received signal strength. The BSs are selected by comparing the power spectrum of the received signal with a preset threshold.

The comparison of RMSEs is shown in Fig.11 and Fig.12, where *Algorithm* 1 is the proposed method, *Algorithm* 2 is the IMMPF proposed in [25] with three motion models and only LOS channel model, *Algorithm* 3 is the MKF algorithm proposed in [16] with CV motion model and mixed LOS/NLOS channel models, *Algorithm* 4 is a special case of *Algorithm*1 with CV and CT motion models and mixed LOS/NLOS channel models, and *Algorithm* 5 is also a special case of *Algorithm*1 with CV and CA motion models and

mixed LOS/NLOS channel models. The PCRLB of position estimation for *Algorithm* 1 is calculated as

$$PCRLB(k) = \sum_{j=1}^{3} \left[\mu_j(k) PCRLB_j(k) \right], \qquad (42)$$

where

$$PCRLB_j(k) = \sqrt{J_{j,(1,1)}^{-1}(k) + J_{j,(4,4)}^{-1}(k)}. \qquad (43)$$

In Fig.11, it can be seen that *Algorithm*1 outperforms other compared algorithms, and the RMSE of *Algorithm*1 is very close to the PCRLB. Especially, at the 200*th* second, about 50% reduction of error relative to the nearest case. Although three motion models are considered in *Algorithm*2, the method can not adaptively compensate the large distance difference offset without LOS/NLOS channel tracking, while the performance of *Algorithm*3 is severely degraded under the conditions of CA and CT motion models because only CV motion model is considered in the method. The position estimation accuracy of two-motion-model methods are much better than that of CV-only method. It can be noticed that *Algorithm*5 has slightly better performance in CA movement while *Algorithm*4 has lower estimation errors in CT movement. Fig.12 shows the comparison of distance difference offset estimation performance. *Algorithm*2 and *Algorithm*3 are not considered in this comparison, because the different offsets are not estimated for the two algorithms. Compared with two-motion-model schemes, *Algorithm*1 can provide more accurate estimates of the distance difference offset. Therefore, the target tracking performance is improved when both the motion and channel model are accurately estimated. The average improvement over the whole time is larger than 40%.

Finally, the computational complexity is assessed in terms of average computation time and is shown in Table I. In the simulation, the total observation time is 550 seconds. The computation time of the proposed *Algorithm*1 is higher than the other algorithms, but it is still acceptable for real-time tracking. Besides, the proposed algorithm has the highest positioning accuracy, because it considers both multiple motion and channel models that could perfectly describe the trajectory of the mobile target.

TABLE 1. Average computation time of each algorithm for the entire trajectory.

Name	Computational time	RMSEs
Algorithm1	16.115 sec.	24.624 m
Algorithm2	11.743 sec.	82.361 m
Algorithm3	11.153 sec.	64.573 m
Algorithm4	14.528 sec.	45.412 m

VI. CONCLUSION

A mobile localization scheme based on TDOA measurements in mixed LOS/NLOS environments has been proposed in

this paper. The existing three-motion-model schemes with only LOS channel model are not suited for frequently switched LOS and NLOS channel, while the tracking performance of NLOS mitigation schemes with only CV motion model is severely degraded under the conditions of CA and CT motion models. To overcome the problems, we have presented an improved IMMPF algorithm. Considering three motion and two channel models, the proposed algorithm can jointly estimate the target position and channel parameters. The performance of the proposed algorithm has been confirmed by the simulation results. The results show that the proposed algorithm is close to the derived PCRLB bound and outperforms other algorithms.

REFERENCES

[1] C.-H. Chen and K.-T. Feng, "Enhanced distance and location estimation for broadband wireless networks," *IEEE Trans. Mobile Comput.*, vol. 14, no. 11, pp. 2257–2271, Nov. 2015.

[2] P. H. Tseng, Z. Ding, and K. T. Feng, "Cooperative self-navigation in a mixed LOS and NLOS environment," *IEEE Trans. Mobile Comput.*, vol. 13, no. 2, pp. 350–363, Feb. 2014.

[3] N. Ahmed, M. Rutten, T. Bessell, S. S. Kanhere, N. Gordon, and S. Jha, "Detection and tracking using particle-filter-based wireless sensor networks," *IEEE Trans. Mobile Comput.*, vol. 9, no. 9, pp. 1332–1345, Sep. 2010.

[4] Y. Bar-Shalom, X. R. Li, *Estimation and Tracking: Principles, Techniques, and Software*. Boston, MA, USA: Artech House, 1993.

[5] F. Gustafsson and F. Gunnarsson, "Mobile positioning using wireless networks: Possibilities and fundamental limitations based on available wireless network measurements," *IEEE Signal Process. Mag.*, vol. 22, no. 4, pp. 41–53, Jul. 2005.

[6] Y. T. Chan and K. C. Ho, "A simple and efficient estimator for hyperbolic location," *IEEE Trans. Signal Process.*, vol. 42, no. 8, pp. 1905–1915, Aug. 1994.

[7] N. Patwari, J. N. Ash, S. Kyperountas, A. O. Hero, R. L. Moses, and N. S. Correal, "Locating the nodes: Cooperative localization in wireless sensor networks," *IEEE Signal Process. Mag.*, vol. 22, no. 4, pp. 54–69, Jul. 2005.

[8] A. Catovic and Z. Sahinoglu, "The Cramér–Rao bounds of hybrid TOA/RSS and TDOA/RSS location estimation schemes," *IEEE Commun. Lett.*, vol. 8, no. 10, pp. 626–628, Oct. 2004.

[9] S. Tomic, M. Beko, and R. Dinis, "Distributed RSS-AoA based localization with unknown transmit powers," *IEEE Wireless Commun. Lett.*, vol. 5, no. 4, pp. 392–395, Aug. 2016.

[10] L. Taponecco, A. A. D'Amico, and U. Mengali, "Joint TOA and AOA estimation for UWB localization applications," *IEEE Trans. Wireless Commun.*, vol. 10, no. 7, pp. 2207–2217, Jul. 2011.

[11] L. Cong and W. Zhuang, "Hybrid TDOA/AOA mobile user location for wideband CDMA cellular systems," *IEEE Trans. Wireless Commun.*, vol. 1, no. 3, pp. 439–447, Jul. 2002.

[12] G. Wang, H. Chen, Y. Li, and N. Ansari, "NLOS error mitigation for TOA-based localization via convex relaxation," *IEEE Trans. Wireless Commun.*, vol. 13, no. 8, pp. 4119–4131, Aug. 2014.

[13] W. Wang, G. Wang, J. Zhang, and Y. Li, "Robust weighted least squares method for TOA-based localization under mixed LOS/NLOS conditions," *IEEE Commun. Lett.*, vol. 21, no. 10, pp. 2226–2229, Oct. 2017.

[14] Z. Abu-Shaban, X. Zhou, and T. D. Abhayapala, "A novel TOA-based mobile localization technique under mixed LOS/NLOS conditions for cellular networks," *IEEE Trans. Veh. Technol.*, vol. 65, no. 11, pp. 8841–8853, Nov. 2016.

[15] L. Xu, J. Wang, H. Zhang, and T. A. Gulliver, "Performance analysis of IAF relaying mobile D2D cooperative networks," *J. Franklin Inst.*, vol. 354, no. 2, pp. 902–916, Jan. 2017.

[16] L. Yan, Y. Lu, and Y. Zhang, "An improved NLOS identification and mitigation approach for target tracking in wireless sensor networks," *IEEE Access*, vol. 5, pp. 2798–2807, 2017.

[17] G. Hao, S. Sun, and Y. Li, "Nonlinear weighted measurement fusion unscented Kalman filter with asymptotic optimality," *Inf. Sci.*, vol. 299, pp. 85–98, Apr. 2015.

[18] M. S. Arulampalam, S. Maskell, N. Gordon, and T. Clapp, "A tutorial on particle filters for online nonlinear/non-Gaussian Bayesian tracking," *IEEE Trans. Signal Process.*, vol. 50, no. 2, pp. 174–188, Feb. 2002.

[19] P. M. Djuric *et al.*, "Particle filtering," *IEEE Signal Process. Mag.*, vol. 20, no. 5, pp. 19–38, Sep. 2003.

[20] F. Gustafsson *et al.*, "Particle filters for positioning, navigation, and tracking," *IEEE Trans. Signal Process.*, vol. 50, no. 2, pp. 425–437, Feb. 2002.

[21] E. Mazor, A. Averbuch, Y. Bar-Shalom, and J. Dayan, "Interacting multiple model methods in target tracking: A survey," *IEEE Trans. Aerosp. Electron. Syst.*, vol. 34, no. 1, pp. 103–123, Jan. 1998.

[22] W. J. Farrell, "Interacting multiple model filter for tactical ballistic missile tracking," *IEEE Trans. Aerosp. Electron. Syst.*, vol. 44, no. 2, pp. 418–426, Apr. 2008.

[23] C.-Y. Yang, B.-S. Chen, and F.-L. Liao, "Mobile location estimation using fuzzy-based IMM and data fusion," *IEEE Trans. Mobile Comput.*, vol. 9, no. 10, pp. 1424–1436, Oct. 2010.

[24] S. Yousefi, X.-W. Chang, and B. Champagne, "Mobile localization in non-line-of-sight using constrained square-root unscented Kalman filter," *IEEE Trans. Veh. Technol.*, vol. 64, no. 5, pp. 2071–2083, May 2015.

[25] D.-C. Chang and M.-W. Fang, "Bearing-only maneuvering mobile tracking with nonlinear filtering algorithms in wireless sensor networks," *IEEE Syst. J.*, vol. 8, no. 1, pp. 160–170, Mar. 2014.

[26] P. H. Foo and G. W. Ng, "Combining the interacting multiple model method with particle filters for manoeuvring target tracking with a multi-static radar system," *IET Radar, Sonar Navigat.*, vol. 5, no. 7, pp. 697–706, 2011.

[27] K. Yu and E. Dutkiewicz, "NLOS identification and mitigation for mobile tracking," *IEEE Trans. Aerosp. Electron. Syst.*, vol. 49, no. 3, pp. 1438–1452, Jul. 2013.

[28] I. Arasaratnam and S. Haykin, "Cubature Kalman filters," *IEEE Trans. Autom. Control*, vol. 54, no. 6, pp. 1254–1269, Jun. 2009.

[29] H. Van Trees and K. L. Bell, *Bayesian Bounds for Parameter Estimation and Nonlinear Filtering/Tracking*. Hoboken, NJ, USA: Wiley, 2007.

[30] P. Tichavsky, C. H. Muravchik, and A. Nehorai, "Posterior Cramér–Rao bounds for discrete-time nonlinear filtering," *IEEE Trans. Signal Process.*, vol. 46, no. 2, pp. 1386–1395, May 1998.

NAN XIA received the B.Eng. degree in electrical engineering from Dalian Jiaotong University, Dalian, China, in 2006, and the Ph.D. degree in signal and information processing from the Dalian University of Technology, Dalian, in 2012. From 2013 to 2017, he was with The State Radio Monitoring Center, Beijing, China, where he was a Senior Engineer. He was a Postdoctoral Research Scholar with the School of Electrical and Computer Engineering, Georgia Institute of Technology, Atlanta, USA, in 2016. He joined the School of Information Science and Engineering, Dalian Polytechnic University, Dalian, in 2017, as an Associate Professor. His research interest include target localization and tracking in wireless networks.

MARY ANN WEITNAUER (INGRAM) (M'83–SM'03) was a Visiting Professor with Aalborg University, Aalborg, Denmark, from 2006 to 2008, and with Idaho National Labs, in 2010. She is currently a Professor and a Senior Associate Chair with the School of Electrical and Computer Engineering, Georgia Tech, where she has been a Faculty Member for 29 years. She has over 20 years of experience in MIMO wireless communications, RF beamforming, MIMO networking, and RF channel modeling. Her research has been focused on the lower three layers of MIMO wireless networks that have real or distributed antenna arrays, at microwave and millimeter-wave frequencies. Many results are demonstrated on a 20-node network of software-defined radios in practical environments and topologies. She has authored or co-authored over 200 refereed journal and conference papers. She received four best paper awards in conferences. She held the Georgia Tech ADVANCE Professorship for the College of Engineering, from 2006 to 2012. She was an Associate Editor of the IEEE Transactions on Mobile Computing, from 2009 to 2012.

● ● ●